Journal of Catalysis 264 (2009) 31–43

Contents lists available at ScienceDirect

Journal of Catalysis

journal homepage: www.elsevier.com/locate/jcat

Hydrodesulfurization of dibenzothiophene, 4,6-dimethyldibenzothiophene, and their hydrogenated intermediates over Ni–MoS_2/γ-Al_2O_3

Huamin Wang [1], Roel Prins *

Institute of Chemical and Bioengineering, ETH Zurich, Wolfgang Paulistrasse 10, 8093 Zurich, Switzerland

ARTICLE INFO

Article history:
Received 27 January 2009
Revised 6 March 2009
Accepted 9 March 2009
Available online 17 April 2009

Keywords:
Hydrodesulfurization
HDS
Dibenzothiophene
4,6-Dimethyldibenzothiophene
Hydrogenated intermediates
Mechanism
Kinetics
Inhibition by H_2S
Effect of piperidine
Sulfided NiMo/γ-Al_2O_3

ABSTRACT

The rate constants of all reaction steps in the hydrodesulfurization (HDS) of dibenzothiophene (DBT), 4,6-dimethyldibenzothiophene (DMDBT), and their tetra- and hexahydro intermediates TH(DM)DBT and HH(DM)DBT over Ni–MoS_2/γ-Al_2O_3 were determined. DBT, THDBT, DMDBT, and THDMDBT underwent desulfurization by hydrogenolysis of both C–S bonds, while HHDBT and HHDMDBT underwent desulfurization by cleavage of the aryl C–S bond by hydrogenolysis, followed by cleavage of the cycloalkyl C–S bond by elimination as well as by hydrogenolysis. Ni promoted the C–S bond breakage of DBT, THDBT, and HHDBT strongly, but promoted the (de)hydrogenation only weakly. The methyl groups suppressed the desulfurization in the order DMDBT > THDMDBT > HHDMDBT and promoted hydrogenation. These different degrees of steric hindrance are due to the hydrogenation of a phenyl ring, which makes the THDBT and HHDBT rings flexible. H_2S strongly inhibited the desulfurization rates in the order (DM)DBT > TH(DM)DBT > HH(DM)DBT, but inhibited the (de)hydrogenation rates only slightly. 2-Methylpiperidine inhibited the hydrogenation of all molecules.

1. Introduction

An ever-increasing number of countries have announced that they will introduce stringent legislation regarding the maximum permitted level of sulfur in gasoline and diesel automotive fuels in order to abate air pollution. Sulfur is removed by hydrodesulfurization (HDS) and to attain the required low levels of sulfur, it is necessary to improve the HDS catalyst and the HDS process. Therefore a better understanding of the reaction mechanisms and the HDS kinetics of sulfur-containing molecules is required. Dibenzothiophene (DBT) and its alkylated derivates, especially at the 4 and 6 positions (4,6-dimethyldibenzothiophene, DMDBT), are among the molecules present in the fuel which are very difficult to desulfurize and which cause problems in deep HDS, the removal of large quantities of sulfur from fuel [1–6]. The mechanisms and kinetics of HDS have been studied extensively and DBT and alkyl-substituted DBT have been shown to undergo HDS by two reaction pathways, direct desulfurization (DDS) and hydrogenation (HYD). DDS leads to the formation of biphenyls, while HYD yields tetrahydro (TH), hexahydro (HH), and dodecahydro (DH) sulfur-containing intermediates, which are desulfurized to cyclohexylbenzenes (CHBs) and bicyclohexyls (BCHs) (Scheme 1) [1–11]. The HYD pathway is about equally fast for DBT and DMDBT, but the DDS pathway is much faster for DBT than for DMDBT and much faster than the HYD pathway [4,8–12]. As a result, DBT reacts mainly by the DDS pathway and DMDBT reacts mainly by the slower HYD pathway. This low DDS reactivity of DMDBT over MoS_2 catalysts is due to the steric hindrance of the alkyl groups at the 4 and 6 positions, which are close to the sulfur atom and prevent the σ-binding of the sulfur atom with the catalytic site [1–6,13–15]. The alkyl groups do not hinder the π adsorption of DMDBT on the catalyst surface in the HYD reaction [8,11,16], but decrease the rate of the final desulfurization in the HYD pathway [11].

Most HDS results have been obtained from studies of DBT or DMDBT. The information derived from studying only the parent molecule in a complex kinetic scheme (Scheme 1) has, however, a limited value. To obtain reliable kinetic data, the reactions of the intermediates should be studied as well. At the same time, this indicates how the sulfur atoms of the hydrogenated intermediates are removed. The recent synthesis of the tetrahydro and hexahydro intermediates of DBT and DMDBT [17,18] enabled the study of the mechanisms and kinetics of the HDS of DMDBT and DBT and their intermediates over MoS_2/γ-Al_2O_3 [18,19].

The actual catalysts used in the industry, now and in the near future, contain Co or Ni in addition to the active MoS_2 phase, because the Ni and Co atoms improve the catalytic activity of the

* Corresponding author. Fax: +41 44 6321162.
E-mail address: prins@chem.ethz.ch (R. Prins).
[1] Present address: Dept. Chem. Engineering, University of California, Berkeley.

0021-9517/$ - see front matter © 2009 Elsevier Inc. All rights reserved.
doi:10.1016/j.jcat.2009.03.011

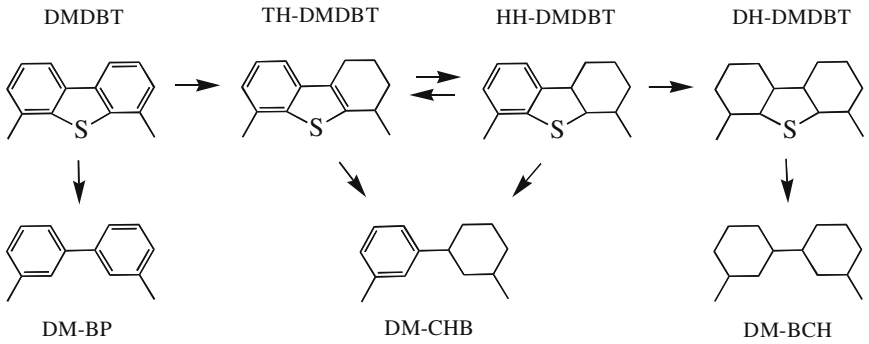

Scheme 1. Reaction network of the HDS of DMDBT.

MoS_2 catalyst several fold [2–6]. This has been ascribed to a promotion of the DDS pathway and of the final sulfur-removal step in the HYD pathway [11]. To determine the role of the promoter, we studied the HDS of DBT and DMDBT, and their hydrogenated intermediates (THDBT, HHDBT, THDMDBT, and HHDMDBT) over a Ni–MoS_2/γ-Al_2O_3 catalyst at 300 °C and at 3.0 and 5.0 MPa. These HDS experiments were possible only because of the development of a synthesis route that allowed us to obtain a sufficient amount (10–20 g) of THDMDBT [20]. Since actual fuels contain not only sulfur-containing molecules, but also nitrogen-containing compounds, we studied the HDS in the presence of H_2S and 2-methylpiperidine as a model nitrogen-containing compound. Our aim was to reveal the reaction mechanisms, determine the kinetics, investigate the inhibition effects of H_2S and 2-methylpiperidine, and compare the HDS of DBT and DMDBT over a Ni–MoS_2 catalyst with the HDS over a MoS_2 catalyst.

2. Experimental

A sulfided Ni–MoS_2/γ-Al_2O_3 catalyst (3 wt% Ni and 8 wt% Mo) was prepared by incipient wetness impregnation of γ-Al_2O_3 (Condea, pore volume 0.5 cm^3/g, specific surface area 230 m^2/g). The catalyst was crushed and sieved to a 230-mesh (<0.063 mm) particle size. Further details of the catalyst preparation can be found elsewhere [18].

Reactions were carried out in continuous mode in a heated fixed-bed inconel reactor. The catalyst was sulfided in situ with 10% H_2S in H_2 (50 ml/min) at 400 °C and 1.0 MPa for 4 h. All the experiments were performed at 300 °C. The gas-phase feed consisted of 1 kPa reactant (DBT, THDBT, HHDBT, DMDBT, THDMDBT, or HHDMDBT), 130 kPa toluene (as solvent), 8 kPa dodecane (as GC reference), 0 or 35 kPa H_2S, and 4.8 or 2.8 MPa H_2. In some experiments 1 kPa 2-methylpiperidine (MPi) was added to the feed to decrease the speed of the reaction and to study the influence of a nitrogen-containing compound. 2-Methylpiperidine was preferred over piperidine, because piperidine is known to react to *N*-pentylpiperidine, which complicates the determination of the mass balance.

The reaction products were analyzed off-line, as described elsewhere [19]. Weight time [21] was defined as the ratio of the catalyst weight to the molar flow to the reactor (1 g min/mol = 0.15 g h/l at 300 °C and at 5.0 MPa). The weight time was changed by varying the flow rates of the liquid and the gaseous reactants, while keeping their ratio constant. Each series of experiments over a fresh catalyst started with a stabilization period of at least 15 h (overnight) at the highest weight time. During two weeks of operation almost no deactivation of the catalyst was observed. A single experiment lasted for 12–24 h.

DBT (Acros), DMDBT (Acros), and 2-methylpiperidine (Acros) were all used as purchased. THDBT was synthesized in two steps according to the method of DiCesare et al. [22]. HHDBT was produced by hydrogenation of THDBT with zinc and trifluoroacetic acid at room temperature [19]. THDMDBT was synthesized by a four-step procedure, in which 2-bromo-3-methylcyclohexanone was synthesized by the conjugate addition of trimethylaluminum to 2-bromo-2-cyclohexen-1-one with copper bromide as a catalyst, coupled with 2-methylthiophenol, and the product was annulated to THDMDBT with a polyphosphoric acid catalyst [20]. HHDMDBT was prepared in an autoclave by hydrogenation of DMDBT over a Pd/C catalyst, and then separated by column chromatography [7,17,18].

3. Results

3.1. HDS of DBT

All the HDS experiments over the Ni–MoS_2/γ-Al_2O_3 catalyst were performed at 300 °C and usually at 3 MPa, because at higher temperature and H_2 pressure, the conversions of the tetrahydro and hexahydro intermediates of DBT and DMDBT over the Ni–MoS_2 catalyst were too high. To enable a comparison with the results of our previous experiments over the less active MoS_2/γ-Al_2O_3 catalyst [19], obtained at 5.0 MPa, an HDS experiment was also performed for each reactant at 5.0 MPa and 35 kPa H_2S. The studies at 3.0 MPa were carried out in the absence and presence of H_2S and MPi to determine their inhibition of the HDS kinetics. Figs. 1 and 2 show the yield-time dependencies and the product selectivities in the HDS of DBT under different conditions. Assuming pseudo first-order kinetics, we calculated the initial rate constants k_{DBT} from the overall conversion of DBT at short weight time. By considering the selectivities, it was also possible to calculate the initial rate constants of hydrogenation and desulfurization of DBT (k_{HYD} and k_{DDS}, respectively). The results are given in Table 1.

Five products were observed in the HDS of DBT at 5.0 MPa and 35 kPa H_2S (Fig. 1): biphenyl (BP), the product of the DDS pathway, tetrahydro-DBT (THDBT) and hexahydro-DBT (HHDBT), the intermediates of the HYD pathway, and cyclohexylbenzene (CHB) and bicyclohexyl (BCH), the final products of the HYD pathway. The selectivity of BP formation, that is, the selectivity for the DDS pathway, was 72% and remained almost constant during the reaction (Fig. 1B). This shows that the DDS route is much easier than the HYD route for the HDS of DBT, and that BP is not further hydrogenated. The selectivities to THDBT and HHDBT decreased with increasing weight time and were very low at high weight time, indicating that these intermediates reacted quickly to the desulfurized product molecules CHB and BCH.

At 3.0 MPa and 0 kPa H_2S, DBT reacted very rapidly (Fig. 2A); BP was the main product with a constant selectivity of 95% (Fig. 2B). Addition of 35 kPa H_2S caused a strong decrease in the conversion (Fig. 2A), mainly due to the decrease in the formation of BP

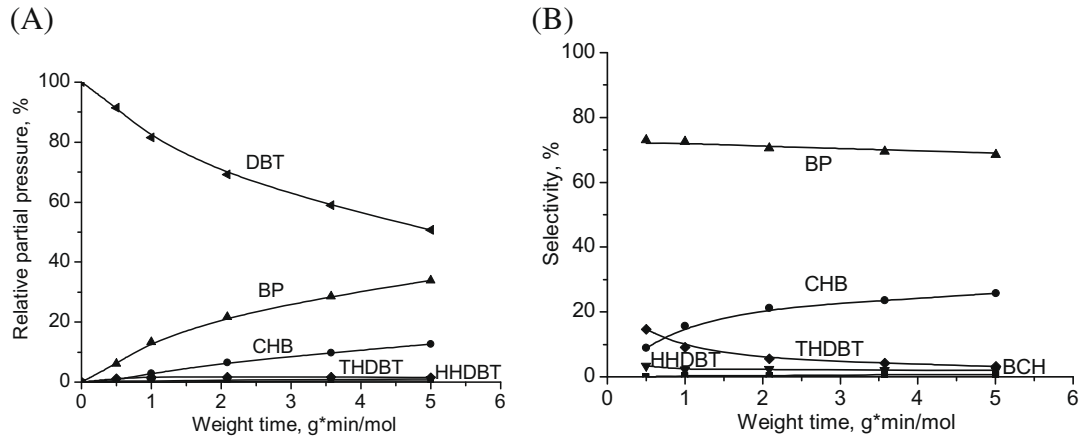

Fig. 1. Relative partial pressure of reactant and products (A) and product selectivities (B) of the HDS of DBT as a function of weight time at 300 °C, 5.0 MPa, and 35 kPa H_2S.

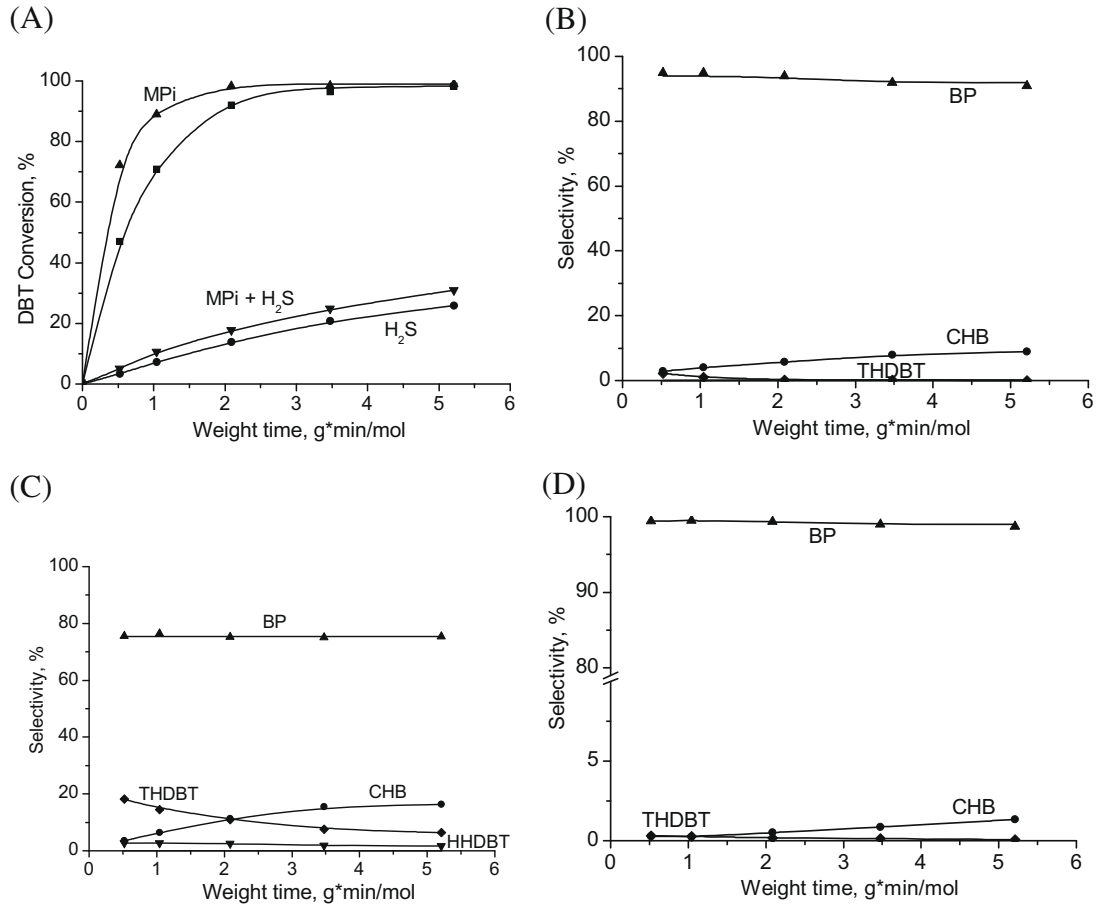

Fig. 2. HDS of DBT at 300 °C and 3.0 MPa. (A) Conversion of DBT in the absence of H_2S and MPi (■), in the presence of 35 kPa H_2S (●), in the presence of 1 kPa MPi (▲), and in the presence of both 35 kPa H_2S and 1 kPa MPi (▼). Product selectivities in the absence of H_2S and MPi (B), in the presence of 35 kPa H_2S (C), and in the presence of 1 kPa MPi (D).

(Fig. 2C). As a consequence, k_{DDS} was about 24 times lower at 35 than at 0 kPa H_2S (Table 1), while k_{HYD} was only four times lower. The conversion of DBT was higher (Fig. 2A) and the rate constant k_{DBT} was about twice as high in the presence of 1 kPa MPi than in the absence of MPi (Table 1). This was due to the promotion of the desulfurization of DBT by MPi. The rate constant k_{DDS} was twice as high in the presence than in the absence of 1 kPa MPi, whereas k_{HYD} decreased by a factor of 15. As a result, BP represented 99% of the reaction products (Fig. 2D).

3.2. HDS of DMDBT

DMDBT reacted 2.4 times slower than DBT at 5.0 MPa and 35 kPa H_2S (Fig. 3), and six products were observed: dimethylbiphenyl (DMBP), the product of the DDS pathway, THDMDBT, HHDMDBT, and (a trace of) 4,6-dimethyldodecahydrodibenzothiophene (DHDMDBT), the intermediates of the HYD pathway, and 3,3′-dimethylcyclohexylbenzene (DMCHB) and 3,3′-dimethylbicyclohexyl (DMBCH), the final products of the HYD

Table 1
Rate constants for the HDS of DBT, THDBT, and HHDBT over Ni–MoS_2/γ-Al_2O_3 at 300 °C.

Reactant	P_{total} (MPa)	P_{H2S} (init) kPa	P_{Mpi} (init) kPa	Rate constants (kPa mol/(g min)		
				k_{DBT}	k_{HYD}	k_{DDS}
DBT	5.0	35	0	0.17 ± 0.01	0.044	0.13
	3.0	0	0	1.20 ± 0.02	0.060	1.14
	3.0	35	0	0.063 ± 0.003	0.015	0.048
	3.0	0	1	2.36 ± 0.12	0.004	2.32
	3.0	35	1	0.097 ± 0.003	0.003	0.094
				k_{THDBT}	k_{hyd}	k_{dds}
THDBT	5.0	35	0	0.50 ± 0.03	0.35	0.15
	3.0	0	0	0.29 ± 0.02	0.09	0.20
	3.0	35	0	0.13 ± 0.05	0.11	0.019
	3.0	0	1	0.13 ± 0.01	0.039	0.091
	3.0	35	1	0.032 ± 0.001	0.027	0.005
				k_{HHDBT}	k_{dehyd}	k_{dds}
HHDBT	5.0	35	0	0.77 ± 0.01	0.65	0.12
	3.0	0	0	0.39 ± 0.01	0.23	0.15
	3.0	35	0	0.26 ± 0.01	0.23	0.026
	3.0	0	1	0.52 ± 0.05	0.13	0.39
	3.0	35	1	0.20 ± 0.01	0.14	0.051

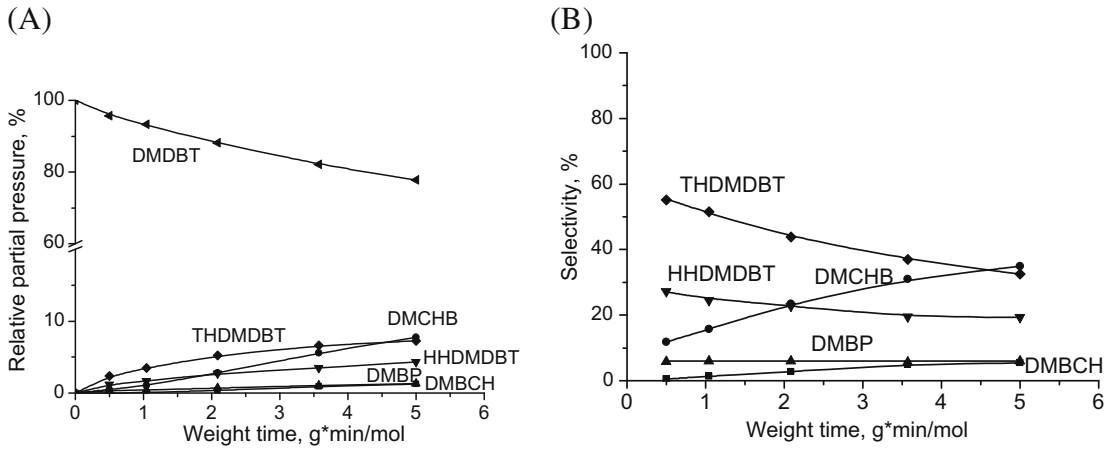

Fig. 3. Relative partial pressure of reactant and products (A) and product selectivities (B) of the HDS of DMDBT as a function of weight time at 300 °C, 5.0 MPa, and 35 kPa H_2S.

Table 2
Rate constants for the HDS of DMDBT, THDMDBT, and HHDMDBT over Ni–MoS_2/γ-Al_2O_3 at 300 °C.

Reactant	P_{total} (MPa)	P_{H2S} (init) kPa	P_{Mpi} (init) kPa	Rate constants (kPa mol/(g min)			
				k_{DMDBT}	k_{HYD}	k_{DDS}	
DMDBT	5.0	35	0	0.054 ± 0.002	0.050	0.004	
	3.0	0	0	0.17 ± 0.01	0.13	0.046	
	3.0	35	0	0.029 ± 0.001	0.026	0.003	
	3.0	0	1	0.049 ± 0.001	0.030	0.019	
	3.0	35	1	0.006 ± 0.001	0.005	0.001	
				$k_{THDMDBT}$	k_{hyd}	k_{dds}	
THDMDBT	5.0	35	0	0.65 ± 0.002	0.60	0.050	
	3.0	0	0	0.58 ± 0.004	0.35	0.23	
	3.0	35	0	0.31 ± 0.02	0.28	0.032	
	3.0	0	1	0.22 ± 0.003	0.12	0.10	
	3.0	35	1	0.091 ± 0.006	0.076	0.014	
				$k_{HHDMDBT}$	k_{dehyd}	k_{dds}	k_{hyd}
HHDMDBT	5.0	35	0	1.33 ± 0.001	1.23	0.10	0.050
	3.0	0	0	1.08 ± 0.02	0.84	0.21	0.029
	3.0	35	0	0.90 ± 0.003	0.80	0.05	0.041
	3.0	0	1	0.56 ± 0.02	0.35	0.18	0.022
	3.0	35	1	0.30 ± 0.001	0.25	0.030	0.031

pathway. In contrast to the high selectivity of BP in the HDS of DBT, the selectivity of DMBP was only 7% (Fig. 3B), demonstrating that the DDS route of DMDBT was strongly suppressed. As a result, k_{DDS} was 13 times lower than k_{HYD} (Table 2). The rate constant k_{HYD}(DMDBT) was slightly higher for DMDBT than that for DBT. THDMDBT and HHDMDBT represented 82% of the reaction

products at the lowest weight time and 52% at the highest weight time, indicating that removal of sulfur from THDMDBT and HHDMDBT is difficult under these conditions. The selectivity of DMCHB and DMBCH increased continuously with weight time, and these molecules were the final products of the HYD pathway.

Also at 3.0 MPa and 0 kPa H_2S, the conversion of DMDBT was much lower than that of DBT (cf. Figs. 2A and 4A). The rate constants k_{DMDBT}, k_{HYD}, and k_{DDS} of DMDBT were seven times lower, twice as high, and 25 times lower than those of DBT, respectively (cf. Tables 1 and 2). This shows that the methyl groups at the 4 and 6 positions promote hydrogenation and strongly inhibit desulfurization. DMCHB was the most abundant compound at $\tau > 1.0$ g min/mol (Fig. 4B), indicating that the further desulfurization of the sulfur intermediates was relatively fast. H_2S strongly

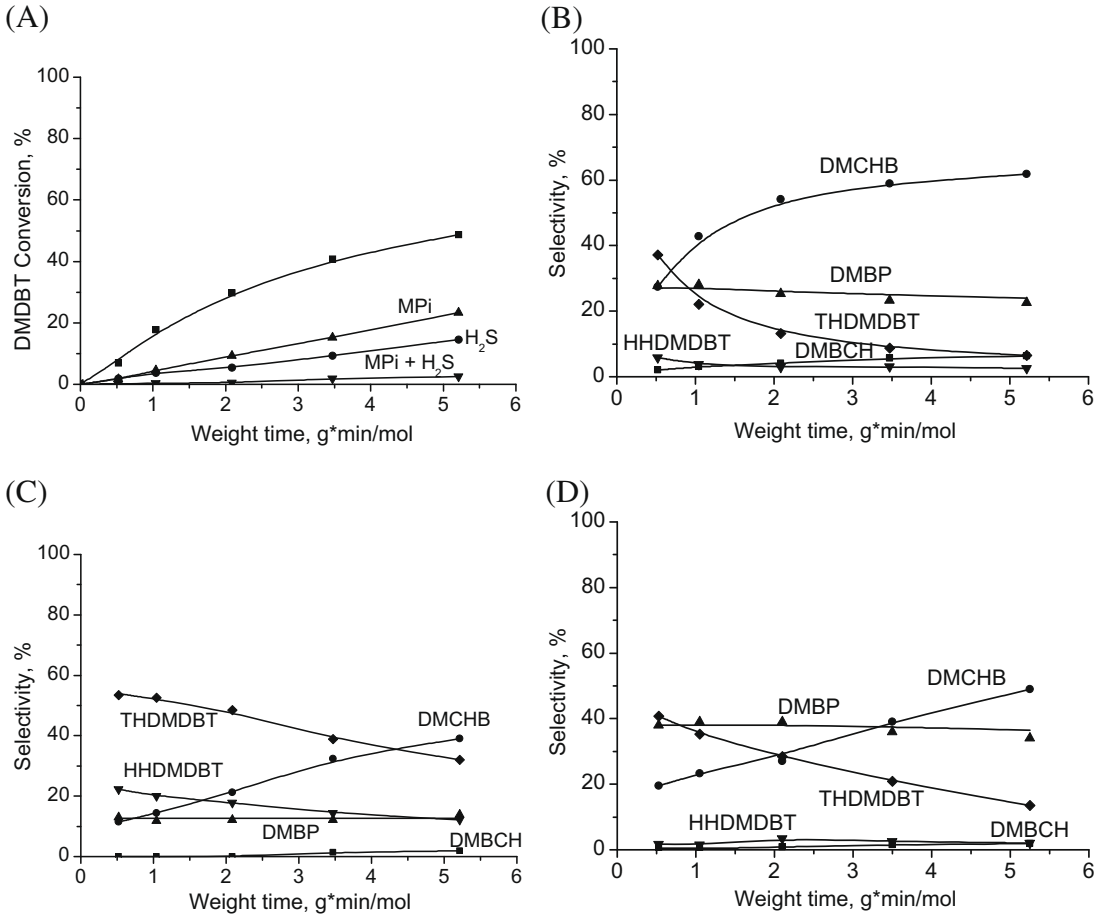

Fig. 4. HDS of DMDBT at 300 °C and 3.0 MPa. (A) Conversion of DMDBT in the absence of H_2S and MPi (■), in the presence of 35 kPa H_2S (●), in the presence of 1 kPa MPi (▲), and in the presence of both 35 kPa H_2S and 1 kPa MPi (▼). Product selectivities in the absence of H_2S and MPi (B), in the presence of 35 kPa H_2S (C), and in the presence of 1 kPa MPi (D).

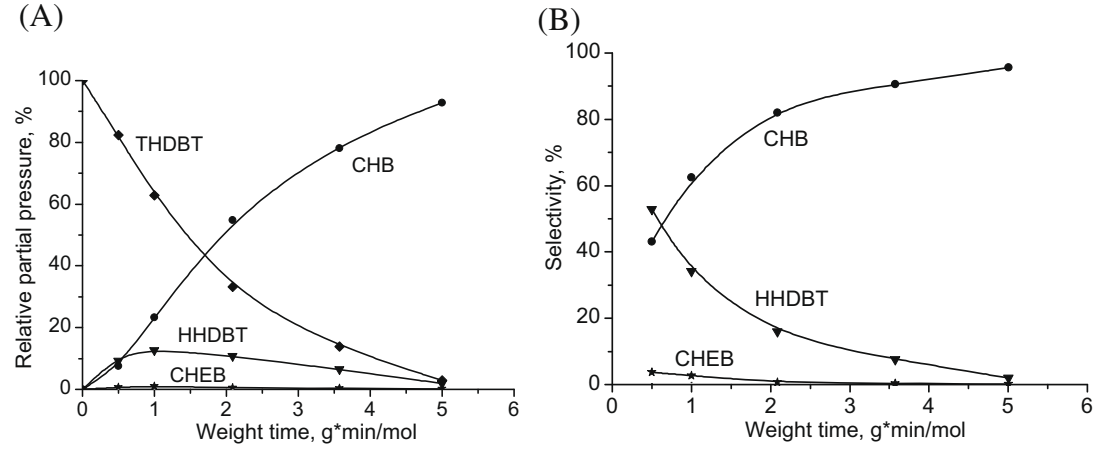

Fig. 5. Relative partial pressure of reactant and products (A) and product selectivities (B) of the HDS of THDBT as a function of weight time at 300 °C, 5.0 MPa, and 35 kPa H_2S.

decreased the conversion of DMDBT. The rate constant k_{DDS} was 15 times lower and k_{HYD} five times lower at 35 than at 0 kPa H_2S. As a result, only 4% of DMDBT was converted at $\tau = 1.0$ g min/mol (Fig. 4A), and the selectivities of the sulfur-containing intermediates were high (Fig. 4C). MPi inhibited the HDS of DMDBT, especially along the HYD pathway. The rate constants k_{DMDBT}, k_{HYD}, and k_{DDS} were 3.7, 4.3, and 2.4 times lower at 1 than at 0 kPa MPi, respectively.

3.3. HDS of THDBT

At 5.0 MPa, and 35 kPa H_2S, THDBT quickly converted to HHDBT, CHB, and cyclohexen-1-yl-benzene (CHEB) (Fig. 5A). All the products behaved as primary products, because they had selectivities higher than zero (70%, 25%, and 5%, respectively) at $\tau = 0$ (Fig. 5B). The rate constant of hydrogenation of THDBT (k_{hyd}) was about eight times higher than that of DBT, whereas its rate constant of desulfurization (k_{dds}) was slightly larger (Table 1).

At 3.0 MPa and 0 kPa H_2S, THDBT reacted fast, but slower than DBT (Fig. 2A). To avoid an excessive number of figures, each composed of four subfigures, the conversions of THDBT, HHDBT, THDMDBT, and HHDMDBT and the selectivities of their HDS products obtained at 3.0 MPa are presented in Figs. SM1, SM2, SM3, and SM4 of Supplementary Material (SM), respectively. The results for THDBT are presented in Fig. SM1A. A substantial amount of CHEB was observed in the HDS of THDBT, with a selectivity of 30% at $\tau = 0$ (Fig. SM1B), indicating that the hydrogenation of CHEB to CHB was not very fast at 3.0 MPa. H_2S strongly inhibited the desulfurization of THDBT and decreased k_{dds} by a factor of about eleven, but k_{hyd} showed little change (Table 1). MPi inhibited both the desulfurization and hydrogenation of THDBT by about 2.2 times (Table 1), which shows that, in contrast to the desulfurization of DBT, MPi did not promote the desulfurization of THDBT. CHEB was the major primary product at $\tau = 0$, with a selectivity of 50% (Fig. SM1D). No BCH was observed in any of the HDS reactions of THDBT (Figs. 5 and SM1), indicating that the further hydrogenation of CHB to BCH was slow under our HDS conditions.

3.4. HDS of THDMDBT

THDMDBT converted quickly to HHDMDBT at 5 MPa and 35 kPa H_2S at short weight time (with 92% selectivity at $\tau = 0$) and then more slowly to other products at higher weight time (Fig. 6). DMCHB behaved as a primary product and DHDMDBT and DMBCH behaved as secondary products. The yield of HHDMDBT first increased and then decreased at $\tau > 1.0$ g min/mol, indicating that HHDMDBT reacted further, by dehydrogenation or desulfurization. The yield-time curves of THDMDBT and HHDMDBT suggest that these molecules tend to reach equilibrium, with a THDMDBT/HHDMDBT ratio of 1.8 at $\tau = 5.2$ g min/mol. The rate constants $k_{THDMDBT}$, k_{hyd}, and k_{dds} of THDMDBT were about twelve times higher than those of DMDBT (Table 2). The rate constant k_{dds} was three times lower and k_{hyd} was 1.7 times higher for THDMDBT than those for THDBT (cf. Tables 1 and 2), again indicating that methyl groups inhibit desulfurization and promote hydrogenation.

At 3.0 MPa and 0 kPa H_2S, THDMDBT reacted fast (Fig. SM2A) and DMCHB was the most abundant product (Fig. SM2B). The rate constants $k_{THDMDBT}$, k_{hyd}, and k_{dds} of THDMDBT were all higher than those of DMDBT, especially k_{dds} (Table 2). The rate constant k_{dds} was slightly higher and k_{hyd} was four times higher for THDMDBT than for THDBT, indicating that the hindrance of the methyl groups was not important under these conditions. 3-Methylcyclohexen-1-yl-3-methylbenzene (DMCHEB) behaved as a primary product, but its selectivity was very low. At 35 kPa H_2S, HHDMDBT was the most abundant product (Fig. SM2C), because H_2S suppressed the desulfurization of THDMDBT by a factor of 7 and caused only a slight decrease in hydrogenation (Table 2). Just as for THDBT, MPi inhibited the desulfurization as well as the hydrogenation of THDMDBT, but the latter to a greater extent than the former (Table 2). DMCHEB behaved as a primary product with low selectivity (Fig. SM2D).

3.5. HDS of HHDBT

HHDBT reacted fast to THDBT (with 83% at $\tau = 0$) at 5 MPa and 35 kPa H_2S (Fig. 7), and CHB and CHEB also behaved as primary products (with low selectivities). The relative partial pressures of the reactant and the products of the HDS of HHDBT (Fig. 7A) and THDBT (Fig. 5A) were very similar at high weight time, with the exception of the higher yield of BCH in the HDS of HHDBT. The dehydrogenation rate constant k_{dehyd} of HHDBT was about 1.8 times higher than the hydrogenation rate constant k_{hyd} of THDBT. The desulfurization rate constant k_{dds} of HHDBT was similar to those of DBT and THDBT (Table 1).

The HDS of HHDBT was also fast at 3.0 MPa and 0 kPa H_2S (Fig. SM3A). The rate constant k_{HHDBT} was higher than k_{THDBT} but smaller than k_{DBT} (Table 1). The rate constant k_{dehyd}(HHDBT) was about 2.5 and four times higher than the k_{hyd} of THDBT and DBT, and k_{dds}(HHDBT) was 1.3 and 7.7 times lower than k_{dds} of THDBT and DBT, respectively. A substantial amount of CHEB was observed

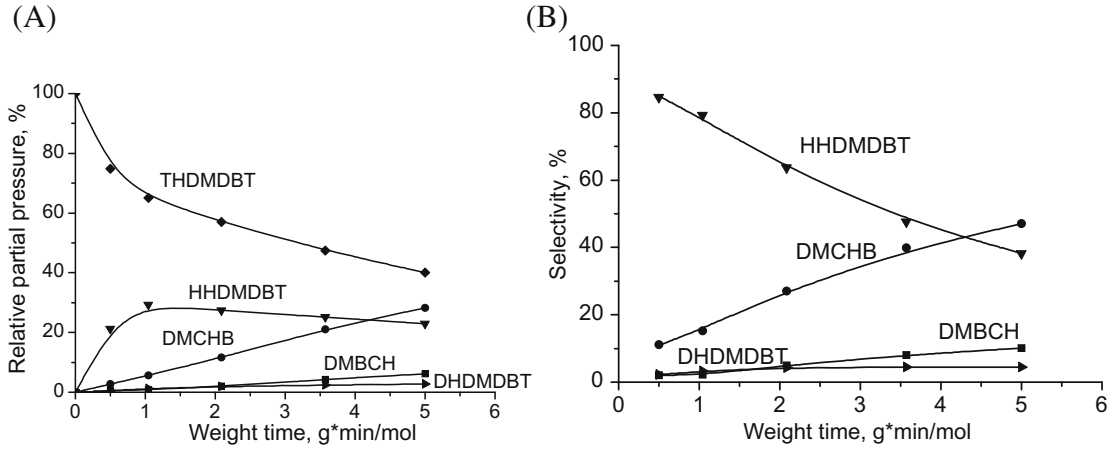

Fig. 6. Relative partial pressure of reactant and products (A) and product selectivities (B) of the HDS of THDMDBT as a function of weight time at 300 °C, 5.0 MPa, and 35 kPa H_2S.

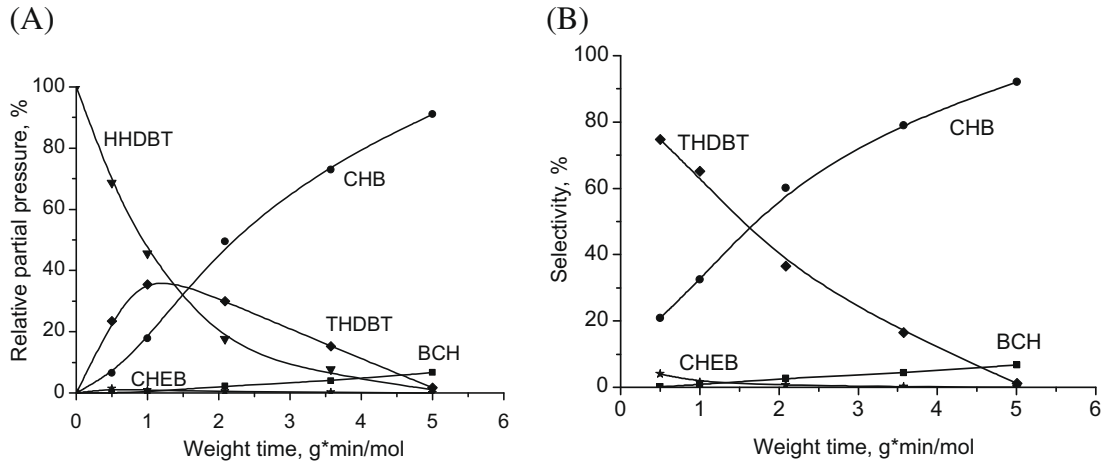

Fig. 7. Relative partial pressure of reactant and products (A) and product selectivities (B) of the HDS of HHDBT as a function of weight time at 300 °C, 5.0 MPa, and 35 kPa H_2S.

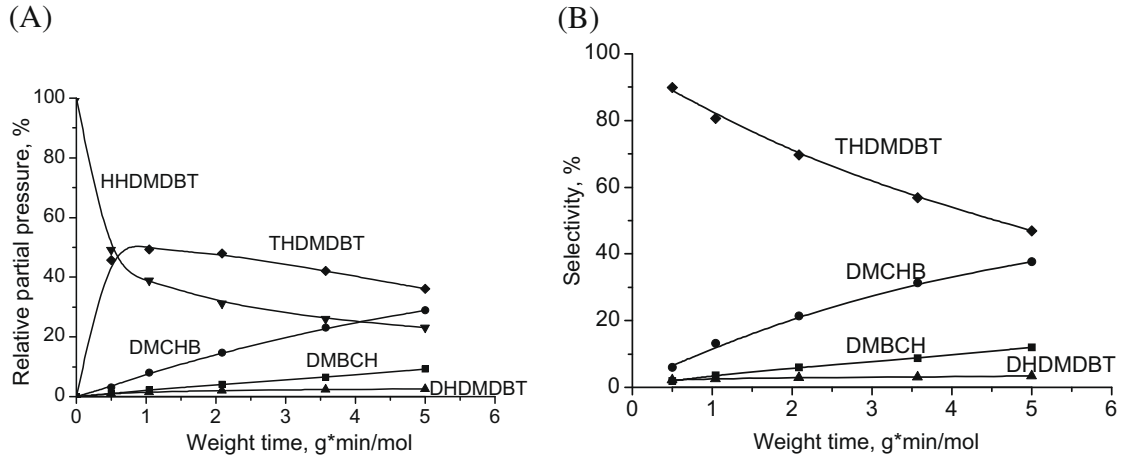

Fig. 8. Relative partial pressure of reactant and products (A) and product selectivities (B) of the HDS of HHDMDBT as a function of weight time at 300 °C, 5.0 MPa, and 35 kPa H_2S.

(Fig. SM3B). H_2S inhibited the desulfurization of HHDBT by a factor of six, but hardly affected its dehydrogenation (Table 1), so that THDBT was the most abundant product at all weight times (Fig. SM3C). The selectivity of CHEB was low, because H_2S inhibited its formation and did not affect its hydrogenation. The effect of MPi on the HDS of HHDBT was very similar to that on the HDS of DBT. The rate constant k_{dds} increased by about 2.6 times after the addition of 1 kPa MPi, whereas k_{dehyd} was about 1.8 times lower (Table 1); as a result, k_{HHDBT} increased by about a factor of 1.3. CHEB was the most abundant primary product at low weight time (Fig. SM3D).

3.6. HDS of HHDMDBT

HHDMDBT reacted the fastest of the six compounds that we studied at 5 MPa and 35 kPa H_2S, with high selectivity to THDMDBT at short weight time (Fig. 8). The yield-time curves of THDMDBT and HHDMDBT suggest that these molecules tend to reach equilibrium, with a THDMDBT/HHDMDBT ratio of 1.6 at τ = 5.2 g min/mol, similar to the results for THDMDBT. DHDMDBT and DMCHB had low yields and behaved as primary and secondary products, respectively. The rate constants $k_{HHDMDBT}$, k_{dehyd}, and k_{dds} of HHDMDBT (Table 2) were all about twice as high as $k_{THDMDBT}$, k_{hyd}, and k_{dds} of THDMDBT, respectively. The methyl groups promoted hydrogenation and inhibited desulfurization. Therefore, k_{dds} and k_{hyd} were about 1.2 times smaller and two times larger than those of HHDBT (cf. Tables 1 and 2).

At 3.0 MPa and 0 kPa H_2S, $k_{HHDMDBT}$ was about twice as high as $k_{THDMDBT}$ (Table 2), mainly due to the higher k_{dehyd}(HHDMDBT) compared to k_{hyd}(THDMDBT). Similarly, $k_{HHDMDBT}$ was about 2.8 times higher than k_{HHDBT} (cf. Tables 1 and 2), mainly due to the 3.6 times higher $k_{dehyd}$of HHDMDBT than that of HHDBT. In the presence of H_2S, THDMDBT was always the most abundant product (Fig. SM4C), because H_2S suppressed the desulfurization of HHDMDBT four-fold and the dehydrogenation only slightly (Table 2). MPi decreased the rate constants of HHDMDBT by factors of 1.2 to 2.4 (Table 2) and the dehydrogenation of HHDMDBT to a greater extent than the desulfurization of HHDMDBT. DMCHEB behaved as a primary product with a low selectivity (Fig. SM4D).

4. Discussion

4.1. Reaction rates

The kinetic results of the HDS of DBT and its intermediates at 5.0 MPa and 35 kPa H_2S are presented in Table 1 and combined in Scheme 2, while the results for DMDBT and its intermediates are presented in Table 2 and Scheme 3. Schemes 2 and 3 suggest

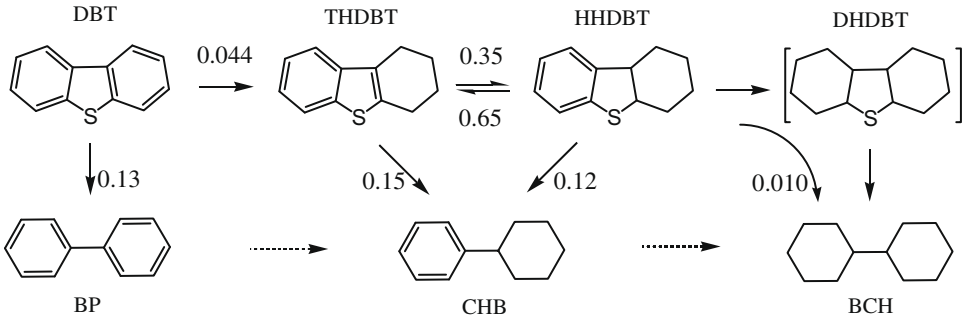

Scheme 2. Rate constants in kPa mol/(g min) in the reaction network of the HDS of DBT over Ni–MoS_2/γ-Al_2O_3 at 300 °C, 5.0 MPa, and 35 kPa H_2S.

that the indicated rate constants are applicable when starting the HDS with (DM)DBT, with TH(DM)DBT, as well as with HH(DM)DBT as the reactant. However, this is true only when there are no differences in the inhibiting effects of these reactants. For instance, the rate equation for the disappearance of DBT is

$$-dP_{DBT}/dt = k'_{DBT}K'_{DBT}P_{DBT}P^{n}_{H2}/[1+\Sigma K'_iP_i] + k''_{DBT}K''_{DBT}P_{DBT}P^{m}_{H2}/[1+\Sigma K''_iP_i],$$

where P_i is the partial pressure of component i, K'_i is its adsorption constant on a DDS site and K''_i is its adsorption constant on an HYD site, k'_{DBT} is the rate constant of DBT on a DDS site and k''_{DBT} is its rate constant on a HYD site, and the summation Σ applies to all sulfur-containing molecules present in the mixture. The rate constants given in Table 1 are lumped rate constants, for instance $k_i(DDS) = k'_iK'_iP^{n}_{H2}/[1+\Sigma K'_iP_i]$. If adsorption of the sulfur-containing molecules cannot be ignored ($\Sigma K_iP_i > 1$), then for instance the lumped rate constant $k_{THDBT}(DDS) = k_{DDS}$ for the DDS of THDBT may depend on the fact if one starts with THDBT or with DBT as the reactant, because in the former case $k_{DDS} = k'_{THDBT}K'_{THDBT}P^{n}_{H2}/[1+K'_{THDBT}P_{THDBT}]$ initially, and in the latter case $k_{DDS} = k'_{THDBT}K'_{THDBT}P^{n}_{H2}/[1+K'_{DBT}P_{DBT}]$.

To check for differences in the adsorption constants of the sulfur-containing molecules, we performed the HDS of a mixture of DMDBT and THDMDBT at 300 °C and 3 MPa. Because THDMDBT does not react back to DMDBT (Fig. SM2), and the yield of THDMDBT from DMDBT is low (Fig. 4) under our experimental conditions, it is not necessary to label one of the two reactants to distinguish semi-quantitatively between the origin of the products in the mixed HDS experiment. The initial partial pressure of DMDBT as well as THDMDBT was 0.5 kPa, so that the total initial pressure of sulfur-containing molecules was 1 kPa, as in all experiments in which only one molecule reacted. Comparison of the results of the mixed experiment with those of the single components showed that the reaction of DMDBT was slowed down by the presence of 0.5 kPa THDMDBT, but that the reaction of THDMDBT was hardly influenced by the presence of DMDBT. For our purpose, to understand the kinetics of the HDS of DMDBT, the inhibition of the reaction of DMDBT to THDMDBT by THDMDBT is of minor importance, because the THDMDBT pressure in the HDS of DMDBT alone is always below 0.05 kPa (Fig. 4A and B). Thus, applying the rate constants presented in Tables 1 and 2 to Schemes 2 and 3 is allowed, as long as they are regarded as being semi-quantitative rather than quantitative.

The hydrogenations of the phenyl rings of DBT were the rate-determining steps in the HYD pathway at 5.0 MPa and 35 kPa H_2S, because the hydrogenation of HHDBT to DHDBT was the slowest step and the hydrogenation of DBT to THDBT was the second slowest step (Scheme 2). The rate constant of the DDS of DBT was about 3.2 times larger than that of the HYD, and thus, the DDS pathway dominates the HDS of DBT over Ni–MoS_2/γ-Al_2O_3. The rate constants of the desulfurization of DBT, THDBT, and HHDBT were similar (0.12 to 0.15 mol/g min at 5 MPa and 0.02–0.05 mol/g min at 3 MPa and 35 kPa H_2S), indicating that the degree of saturation of the molecules is unimportant for C–S bond breaking under these conditions. Only at 3.0 MPa and 0 kPa H_2S the desulfurization of DBT was faster than that of THDBT and HHDBT.

The hydrogenation of THDBT and the dehydrogenation of HHDBT are the fastest reactions in the network of DBT; their rate constants are several times higher than the desulfurization rate constants. These data as well as the reaction profiles of the HDS of THDBT and HHDBT (Figs. 5 and 7) suggest that these two molecules tend toward equilibrium. The ratio of THDBT/HHDBT approached 2.0 at $\tau = 3.6$ g min/mol and decreased to 1.6 at $\tau = 5.2$ g min/mol during the HDS of DBT, THDBT, and HHDBT (Fig. SM5A). According to the rate constants in Table 1, the ratio of k_{dehyd}(HHDBT)/k_{hyd}(THDBT) is 1.9.

The smallest rate constant in the network of the HDS of DMDBT over Ni–MoS_2/γ-Al_2O_3 at 5.0 MPa and 35 kPa H_2S (Scheme 3) was that of the DDS of DMDBT to DMBP (0.004 mol/(g min)), about thirteen times lower than that of the HYD of DMDBT, showing that the HYD pathway is strongly favored in the HDS of DMDBT. The rate constant of the desulfurization of THDMDBT (0.05 mol/(g min)) is thirteen times higher than that of DMDBT, while the rate constant of the desulfurization of HHDMDBT (0.10 mol/(g min)) is 25 times higher than that of DMDBT. This is explained by the smaller steric hindrance by the methyl group at the 4-position for THDMDBT and HHDMDBT compared to that for DMDBT.

The hydrogenation of THDMDBT and the dehydrogenation of HHDMDBT were the fastest reactions in the kinetic network of DMDBT. These data as well as the HDS reaction profiles (Figs. 6 and 8) suggest that both these molecules tend toward equilibrium. Similar to the results of DBT, the ratio THDMDBT/HHDMDBT in the reactions of DMDBT, THDMDBT, and HHDMDBT approached 1.7 at the highest weight time (Fig. SM5B). The ratio of k_{dehyd}(HHDMDBT)/k_{hyd}(THDMDBT) is 2.1, according to the constants given in Table 2. This value is close to that obtained for THDBT and HHDBT, indicating that the equilibrium constant is hardly influenced by the methyl groups.

4.2. Effect of Ni and the methyl groups

A comparison of the rate constants of the HDS network of DBT over Ni–MoS_2/γ-Al_2O_3 (Scheme 2) with the rate constants obtained over MoS_2/γ-Al_2O_3 [19] at 300 °C, 5.0 MPa, and 35 kPa H_2S indicates that the Ni promoter increased the rates of all the steps in the reaction network. Fig. 9 shows the degree of promotion by Ni (defined as the ratio k(NiMo)/k(Mo)) of the desulfurization and the (de)hydrogenation rate constants of the sulfur-containing compounds. The DDS of DBT was promoted 33-fold, but the HYD of DBT was promoted only two-fold. The desulfurization of THDBT was promoted nine-fold and that of HHDBT three-fold. As a result,

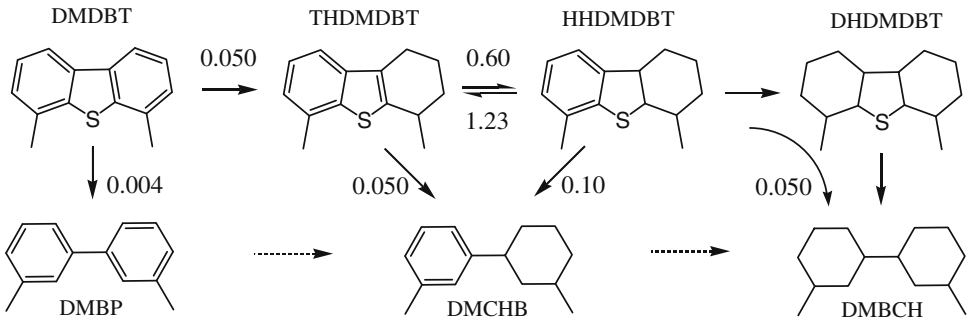

Scheme 3. Rate constants in kPa mol/(g min) in the reaction network of the HDS of DMDBT over Ni–MoS_2/γ-Al_2O_3 at 300 °C, 5.0 MPa, and 35 kPa H_2S.

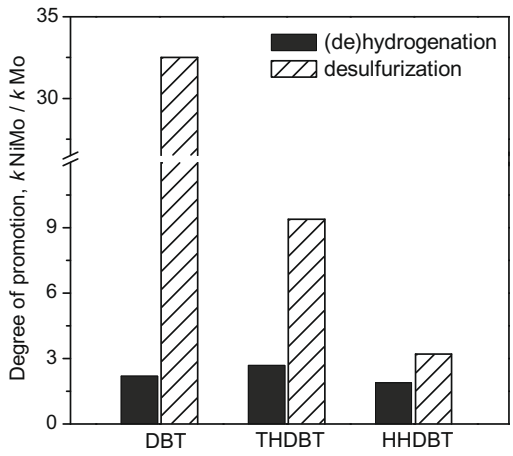

Fig. 9. Degree of promotion by Ni (ratio of the rate constants over Ni–MoS_2/γ-Al_2O_3 and Mo/γ-Al_2O_3) in the hydrogenation of DBT and THDBT and the dehydrogenation of HHDBT (black bars), and in the desulfurization of these three molecules (striped bars).

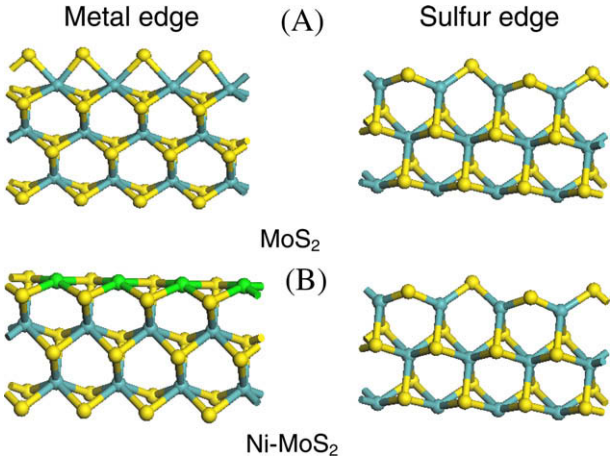

Fig. 10. Location and structure of the Mo atoms at the metal and sulfur edges of a MoS_2 particle and of the Ni atoms at the metal edge of a Ni–MoS_2 particle.

the main HYD product over the Ni–MoS_2 catalyst was CHB (Fig. 1B), whereas over the MoS_2 catalyst THDBT and HHDBT were the main products. The interconversion of THDBT and HHDBT was also faster over the Ni–MoS_2 catalyst than over the MoS_2 catalyst. The promotion of the MoS_2 catalyst by Ni is, therefore, not only due to the faster DDS of DBT, but also due to the faster desulfurization of the hydrogenated intermediates in the HYD pathway. The degree of Ni promotion of the desulfurization is in the order DBT > THDBT > HHDBT (Fig. 9).

Until a decade ago it was generally believed that all reactions taking place during hydrodesulfurization and other hydrotreating reactions take place at coordinatively unsaturated metal sites (CUS) [3,23–25]. The stronger these reactions were inhibited by H_2S, the more sulfur vacancies were supposed to be involved in the catalytic site and the larger the degree of unsaturation of the corresponding metal atom was supposed to be. With the advent of Density Functional Theory (DFT) in hydrodesulfurization science around 2000, it became clear, however, that Mo–S bonds are very strong, and that a large amount of energy is needed to create coordinatively unsaturated Mo sites. Under hydrodesulfurization conditions ($H_2S/H_2 = 10^{-3}$–10^{-1} at 573–673 K), the $(10\bar{1}0)$ edges of MoS_2 particles, the so-called metal edges, therefore do not contain Mo atoms on top of a square of four sulfur atoms, as originally believed, but contain Mo atoms that are trigonal-prismatically coordinated by six sulfur atoms. Also, Mo atoms at the $(\bar{1}010)$ edges, the so-called sulfur edges, are not trigonal-prismatically coordinated by six sulfur atoms, but are tetrahedrally coordinated by four sulfur atoms (Fig. 10A) [26–28]. Because the trigonal-prismatically coordinated Mo atoms are fully coordinated, only the tetrahedrally coordinated Mo atoms play a role in catalysis.

According to the DFT calculations, the Co and Ni promoter atoms at the edges of the MoS_2 crystals have a different structure than the edge Mo atoms [26–29]. The most recent DFT calculations show that under HDS conditions, the Ni atoms are located at the metal edges surrounded by four sulfur atoms in a square-planar coordination (Fig. 10B) as well as at the sulfur edges in a tetrahedral coordination (similar to Mo atoms at the sulfur edges of MoS_2, cf. Fig. 10A) or in a square-planar sulfur coordination [29]. The tetrahedral Mo atoms at the surface of the MoS_2 and Ni–MoS_2 catalyst are less accessible for a sulfur-containing molecule than the square-planar Ni atoms at the surface of the Ni–MoS_2 catalyst. Thus, hydrogenation of DBT alleviates the steric hindrance on the Mo sites to a greater extent than on the Ni sites.

The rate constants of the hydrogenation of DMDBT, THDMDBT, and HHDMDBT and of the dehydrogenation of HHDMDBT were somewhat higher than the corresponding rate constants in the DBT network (Fig. 11). This shows that the methyl groups promote the hydrogenation of the aromatic ring (with π adsorption, flat on the catalyst surface), probably by electron donation. The rate constants of the desulfurization of DMDBT, THDMDBT, and HHDMDBT were about 33, 3, and 1.2 times smaller than those of DBT, THDBT, and HHDBT, respectively (Fig. 11), because of the steric hindrance of the σ adsorption (perpendicular to the catalyst surface) in the desulfurization of DMDBT, THDMDBT, and HHDMDBT. The weaker suppression of THDMDBT and HHDMDBT is due to the fact that the hydrogenation of the phenyl ring allows the methyl group to rotate away from the C–S–C plane, and this is especially true for the

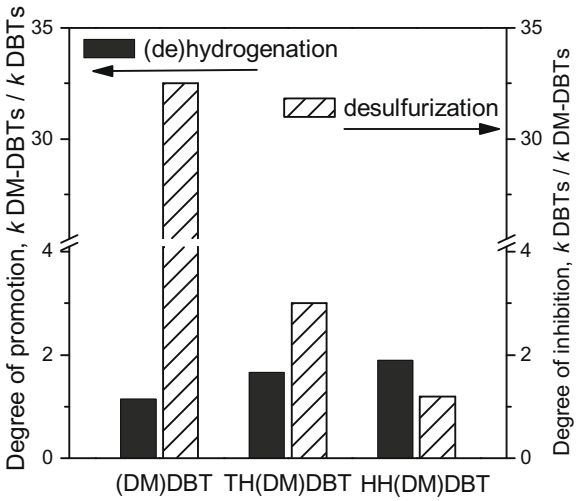

Fig. 11. Effect of the methyl groups in the 4 and 6 positions (ratio of the rate constants of DM-DBTs and DBTs for promotion, the reverse for inhibition) on the hydrogenation of (DM)DBT and TH(DM)DBT, the dehydrogenation of HH(DM)DBT (black bars), and the desulfurization of these three molecules (striped bars).

cyclohexyl ring of HHDMDBT. Consequently, even metal atoms coordinated by several sulfur atoms can bind the hydrogenated intermediates via the sulfur atom, and breaking of the C–S bond speeds up.

4.3. Effect of H_2S, MPi, and H_2 pressure

The effects of H_2S and MPi on the HDS of DBT, DMDBT, and their tetrahydro and hexahydro intermediates were investigated at 3 MPa. Several of the results obtained for DBT and DMDBT have been observed before by others [2–15], but to compare all reactions under the same conditions we had to study the HDS of DBT and DMDBT at 3 MPa as well. The conversions of all six molecules and the selectivities of the desulfurized products decreased when 35 kPa H_2S was introduced, indicating that H_2S strongly inhibited the reaction of these molecules, especially the desulfurization. Fig. 12 shows the degree of inhibition by H_2S (defined as the ratio of the rate constants in the absence and presence of H_2S) of the hydrogenation and dehydrogenation as well as of the desulfurization of the sulfur-containing compounds at 0 or 1 kPa MPi. The degree of inhibition by H_2S was 0.09/0.11 = 0.8 for the hydrogenation of THDBT and even suggests a promotion effect, but actually the degree of inhibition was equal to one within the uncertainty of the measurements. H_2S had a minor effect on the hydrogenation and dehydrogenation of most molecules over MoS_2/γ-Al_2O_3 [9,19,30] and Ni–MoS_2/γ-Al_2O_3 (present work). Only the hydrogenation of DBT and DMDBT was inhibited substantially (four- to five-fold) by H_2S over Ni–MoS_2/γ-Al_2O_3 (Fig. 12A).

Previously, hydrogenation was supposed to take place on coordinatively unsaturated metal atoms, that is on sulfur vacancies [3]. To explain the hydrogenation of aromatic molecules such as toluene [31], pyridine [32], aniline [25], DBT and DMDBT [9] by π adsorption, it had to be assumed that sites with multiple vacancies were involved. This, however, seemed to be at odds with the fact that the inhibition of aromatics hydrogenation by H_2S was only moderate. In the past years, STM investigations have shown that so-called brim sites, on the basal planes of MoS_2 right behind the edges (Fig. 10), have a metallic character and can hydrogenate [33,34]. Since the basal planes are fully sulfided, H_2S has no influence on hydrogenation over the MoS_2 catalyst. This explanation has similarities to a proposal that hydrogenation is caused by electrons and protons, instead of by hydrogen atoms, like in the Birch reduction. In the Birch reduction of aromatics, dissolving an alkali metal in liquid ammonia generates electrons and the protons come from the ammonia. DBT could be reduced to THDBT and HHDBT and DMDBT to THDMDBT and HHDMDBT [35]. In the MoS_2 catalyst, the metallic brim sites can reduce the aromatic molecule, and the proton can be delivered by the SH groups at the MoS_2 edges.

Hydrogenation on a Ni–MoS_2 catalyst can take place on brim sites as well as on Ni sites, and the latter seem to be more active. In the presence of H_2S, the Ni sites get covered by sulfur atoms [36] and become inactive, whereas the brim sites retain their activity. This would explain why hydrogenation activity of a Ni–MoS_2 catalyst decreases to that of a MoS_2 catalyst in the presence of a high partial pressure of H_2S [11]. The reason why all hydrogenations of TH(DM)DBT and dehydrogenations of HH(DM)DBT were hardly influenced by H_2S, whereas the hydrogenation of (DM)DBT

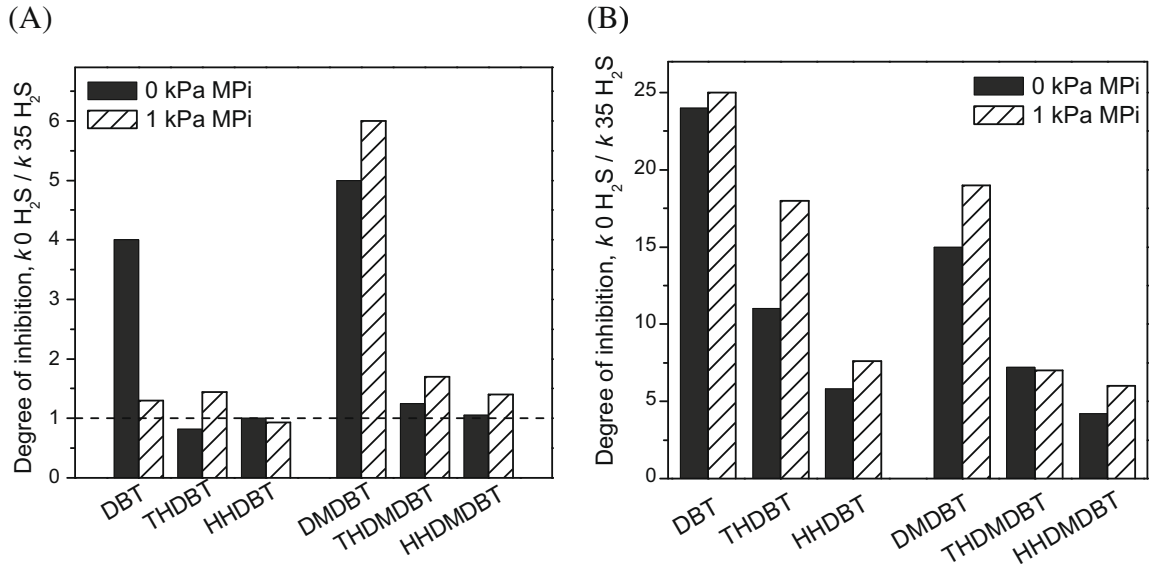

Fig. 12. Degree of inhibition by 35 kPa H_2S (ratio of the rate constants at 0 and 35 kPa H_2S) on the hydrogenation of (DM)DBT and TH(DM)DBT and the dehydrogenation of HH(DM)DBT (A), and on the desulfurization of these six compounds (B) at 3.0 MPa and 0 or 1 kPa MPi.

was moderately inhibited over Ni–MoS_2, might be due to the fact that the hydrogenation of an alkene and corresponding dehydrogenation of an alkane take place on another catalytic site than the hydrogenation of a phenyl ring. The different influence of H_2S on the hydrogenations of benzene and toluene on the one hand and cyclohexene on the other hand was explained this way [23,37]. Whereas the hydrogenation of aromatic molecules takes place on brim sites, alkenes might be hydrogenated on sulfur vacancies, i.e. on accessible metal atoms.

The degree of inhibition of desulfurization by H_2S (Fig. 12B) was much larger than of hydrogenation and dehydrogenation (Fig. 12A) and was in the order (DM)DBT > TH(DM)DBT > HH(DM)DBT (Fig. 12B). This is the reverse of the strength of the M–S σ-bond, because hydrogenation of the phenyl ring increases the electron density on the sulfur atom, and thus increases the interaction with the active sites of the catalyst [38]. Therefore, the more weakly bonded (DM)DBT has more difficulty in competing with H_2S for the sulfur vacancies. Furthermore, the inhibitory effect on DBT and its intermediates is stronger than that on DMDBT and its corresponding intermediates. Even though the methyl groups at the 4 and 6 positions hinder the binding of the sulfur-containing molecule to Mo or Ni atoms that have a high sulfur coordination number, and thus are less accessible, they still seem to enhance the strength of the M–S σ-bond by electron donation, as demonstrated by the higher desulfurization rate of 2,8-DMDBT than that of DBT [13,15,39]. Therefore, molecules with two methyl groups are better able to resist the competitive adsorption of H_2S.

The effect of MPi is complex. The inhibition of the hydrogenation and dehydrogenation of the six compounds by 1 kPa MPi is stronger (Fig. 13A) than the inhibition (or promotion of DBT and HHDBT) of the desulfurization (Fig. 13B). As a result, the selectivities of the desulfurization products are higher in the presence of 1 kPa MPi (Figs. 2, 4, SM1-SM4). This verifies that MPi retards the (de)hydrogenation of DBT and DMDBT and their intermediates over Ni–MoS_2/γ-Al_2O_3 to a greater extent than the desulfurization, as reported before [30,40]. The inhibition of the hydrogenation is most likely due to adsorption of MPi on the metal-like brim sites just behind the edges. DFT calculations have shown that protonation of pyridine by SH groups at the edges of MoS_2 substantially increases the adsorption energy of pyridine on brim sites [41]. DFT calculations on the adsorption of pyridine at the edges of MoS_2 [41] and Ni–MoS_2 [42] showed that pyridine could also be adsorbed on vacancy edge sites by σ bonding of the N atom of pyridine to the metal atom and thus inhibit the direct desulfurization. Analogously, we may expect that the more basic MPi molecules will be strongly adsorbed on brim sites after protonation and on edge vacancies by σ bonding.

The degree of inhibition of the hydrogenation of (DM)DBT, TH(DM)DBT, and dehydrogenation of HH(DM)DBT by MPi is in the order (DM)DBT > TH(DM)DBT > HH(DM)DBT (Fig. 13A), which is the reverse order as over Mo/γ-Al_2O_3 [19]. This might be due to the structure of the Ni–MoS_2 catalyst, which in the absence of H_2S contains Ni atoms at the metal edge that are not covered by sulfur atoms and have a square-planar sulfur coordination with open coordination positions (Fig. 10) [26–29]. Hydrogenation and dehydrogenation occur quickly on a nickel-covered metal edge that is almost free of sulfur. If a MPi molecule adsorbs in the σ mode on such a Ni atom, then the neighboring metal atoms may not allow enough room for the π adsorption of two aromatic rings of (DM)DBT, but enough for the adsorption of the double bond of TH(DM)DBT or the single aromatic ring of HH(DM)DBT. As a result, MPi inhibits the hydrogenation of (DM)DBT to a greater extent than that of TH(DM)DBT and HH(DM)DBT. On the other hand, hydrogenation and dehydrogenation take place on all the edges of the MoS_2 catalysts, regardless of whether they are covered with sulfur or not [33]. This may also explain why H_2S strongly inhibits the hydrogenation of (DM)DBT over a Ni–MoS_2 catalyst but has a weaker effect on a MoS_2 catalyst.

MPi promotes the desulfurization of DBT over the Ni–MoS_2 catalyst at low partial pressure [40,43], but such promotion does not occur over the MoS_2 and Co–MoS_2 catalysts or in the reaction of DMDBT over the Ni–MoS_2 catalyst [19,40]. In agreement with these results, we observed that the desulfurization of DBT and HHDBT was twice as high in the presence of 1 kPa MPi as in the absence of MPi (Table 1). This promotion has been explained by a geometrical effect [43]. The degree of inhibition of desulfurization by MPi is in the order DMDBT > THDMDBT > HHDMDBT (Fig. 13B), the same as the inhibition by H_2S. This must be due to the different σ adsorption constants, as discussed above.

The rate constants of the (de)hydrogenation and desulfurization of DBT and its intermediates were three- to five-fold lower at 3.0 than at 5.0 MPa total pressure (at 300 °C and 35 kPa H_2S), and that

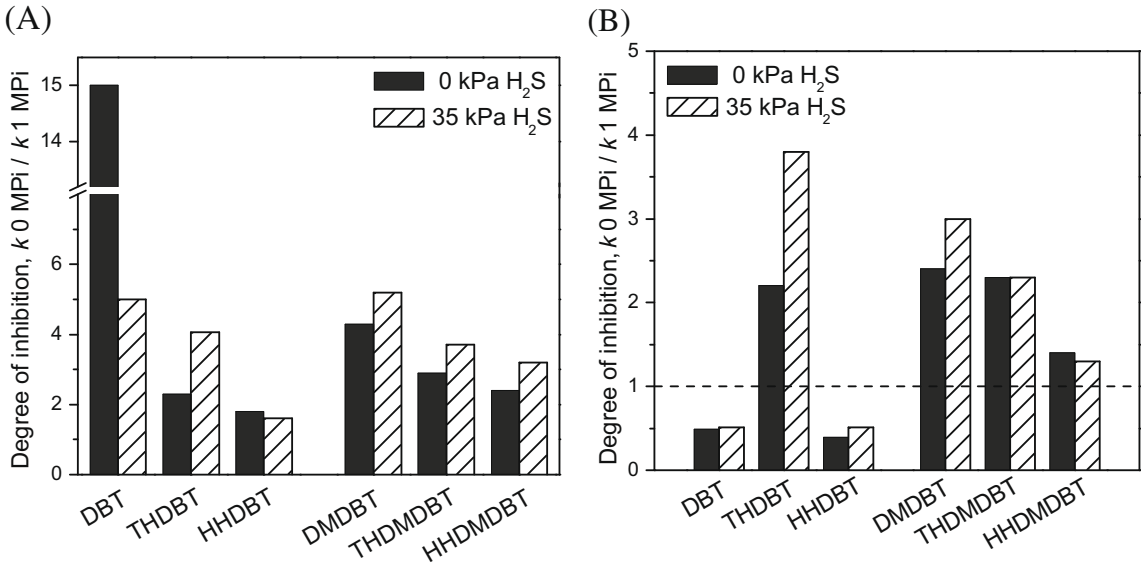

Fig. 13. Degree of inhibition by 1 kPa MPi (ratio of the rate constants at 0 and 1 kPa MPi) on the hydrogenation of (DM)DBT and TH(DM)DBT and the dehydrogenation of HH(DM)DBT (A), and on the desulfurization of these six compounds (B) at 3.0 MPa and 0 or 35 kPa H_2S.

of DMDBT and its intermediates were about 1.4 to two-fold lower (Tables 1 and 2). Furthermore, the rate constants of dehydrogenation of HHDBT and HHDMDBT decreased with decreasing pressure. Thus, hydrogen influences the rate of (de)hydrogenation not only through its partial pressure, but also through its effect on the structure of the catalyst surface. The number of catalytically inactive Ni atom on the catalyst surface, in square-planar sulfur coordination with an additional sulfur atom on top, increases with decreasing H_2/H_2S ratio [32]. Nevertheless, a shift of the (quasi) equilibrium of THDMDBT and HHDMDBT, toward THDMDBT, was observed when the H_2 pressure was decreased from 5.0 to 3.0 MPa. The ratio of THDMDBT/HHDMDBT at 3.0 MPa was around 2.4 to 2.8, as calculated from the rate constants and reaction profiles of the HDS of DMDBT and the two intermediates. This ratio is higher than the ratio (2.0) at 5.0 MPa, most likely because of thermodynamics.

4.4. Mechanism of hydrodesulfurization

Although BP and DMBP behaved as primary products in the HDS of DBT and DMDBT (Figs. 1–4), respectively, it is unlikely that the two C–S bonds of DBT and DMDBT break simultaneously. The DDS of DBT and DMDBT will, therefore, occur in two hydrogenolysis steps, with C–S bond breaking to 2-phenyl-thiophenol for DBT and to 2-(2-methylphenyl)-6-methylthiophenol for DMDBT, followed by C–S bond breaking to BP and DMBP [44]. As explained before [18,19], it is very unlikely that arylthiols such as thiophenol, DBT, and DMDBT undergo desulfurization by hydrogenation to a dihydro intermediate followed by elimination of H_2S, as proposed earlier [9,10].

TH(DM)DBT underwent desulfurization to CHB and CHEB (Figs. 5 and SM1). The yield of CHB increased continuously with weight time, and the yield of CHEB passed through a maximum, indicating that CHEB was an intermediate and was hydrogenated to the final desulfurized product CHB. The selectivity of CHEB at low weight time was much higher in the presence of MPi, because MPi inhibited the hydrogenation of CHEB to CHB. DMCHB was a primary product in the HDS of THDMDBT (Figs. 6 and SM2), whereas DMCHEB had low selectivity (and behaved as a primary product) in the presence of MPi (Fig. SM2D). The hydrogenation of DMCHEB was probably much faster than that of CHEB because of the electron donation by the methyl groups. The reaction of THDBT to CHEB and THDMDBT to DMCHEB may proceed by hydrogenolysis of the two C–S bonds (an aryl C–S bond and a vinyl C–S bond) [19]. Thereafter, fast hydrogenation of CHEB to CHB and of DMCHEB to DMCHB occurs.

CHB and CHEB behaved as primary products in the HDS of HHDBT. The yield-time curves of CHEB and CHB (Figs. 7 and SM3) indicate that CHEB was an intermediate and reacted to CHB. In the HDS of HHDMDBT, DMCHEB was observed only with low selectivity and behaved as a primary product in the presence of MPi (Fig. SM4D), similar to the HDS of THDMDBT. Several reaction pathways are possible in the desulfurization of TH(DM)DBT and HH(DM)DBT, depending on which C–S bond breaks first, and whether elimination or hydrogenolysis of the aliphatic C–S bond occurs, all of which can lead to the simultaneous formation of (DM)CHEB and (DM)CHB. A Density Functional Theory (DFT) calculation of the desulfurization of dihydrobenzothiophene over a Mo_3S_9 cluster showed that the activation energy for hydrogenolysis of the aryl C–S bond in dihydrobenzothiophene is lower than that for breaking the alkyl C–S bond [45]. Cristol et al. calculated a negligible difference in the energy of 2-ethylbenzenethiolate and 2-phenylethanethiolate, the products of alkyl and aryl C–S bond breaking of dihydrobenzothiophene [46]. Dihydro-benzothiophene is similar to HHDBT, with one part of the molecule being aromatic and the other part being aliphatic. Therefore, the desulfurization of HH(DM)DBT over Ni–MoS_2/γ-Al_2O_3 may well take place by hydrogenolysis of the aryl C–S bond, followed by cleavage of the cycloalkyl C–S bond of the resulting thiol by elimination to (DM)CHEB and by hydrogenolysis to (DM)CHB. The selectivity of CHEB over Ni–MoS_2/γ-Al_2O_3 was higher than that over MoS_2/γ-Al_2O_3 at 5.0 MPa and 35 kPa H_2S, possibly because elimination is favored over Ni–MoS_2/γ-Al_2O_3.

5. Conclusions

The mechanism of the desulfurization of DBT and its hydrogenated intermediates (THDBT and HHDBT) over Ni–MoS_2/γ-Al_2O_3 is similar to that over MoS_2/γ-Al_2O_3, and to that of DMDBT and its intermediates (THDMDBT and HHDMDBT) over Ni–MoS_2/γ-Al_2O_3. DBT, THDBT, DMDBT, and THDMDBT undergo desulfurization by hydrogenolysis of both C–S bonds. HHDBT and HHDMDBT undergo desulfurization by cleavage of the aryl C–S bond by hydrogenolysis, and then cleavage of the cycloalkyl C–S bond by elimination as well as by hydrogenolysis.

The rate constants of all the steps of the kinetic networks of the HDS of DBT and DMDBT were measured. Ni promoted the desulfurization of DBT, THDBT, and HHDBT (DBT > THDBT > HHDBT), but hardly promoted their (de)hydrogenation. The methyl groups at the 4 and 6 positions of DMDBT, THDMDBT, and HHDMDBT suppressed their desulfurization by steric hindrance in the order DMDBT > THDMDBT > HHDMDBT and promoted hydrogenation. These different degrees of steric hindrance are due to the hydrogenation of a phenyl ring, which makes the THDBT and HHDBT rings flexible, especially the cyclohexyl ring of HHDBT.

H_2S strongly inhibited the rates of the desulfurization of the six molecules in the order (DM)DBT > TH(DM)DBT > HH(DM)DBT, but affected their (de)hydrogenation only slightly. DMDBT and its intermediates were less affected because of electron donation of methyl groups. MPi inhibited the (de)hydrogenation of the six molecules in the order (DM)DBT > TH(DM)DBT > HH(DM)DBT, which can be explained by the special structure of the Ni–MoS_2 catalyst. MPi promoted the desulfurization of DBT and HHDBT, whereas it inhibited that of THDBT and DMDBT and its intermediates. The promotion effect can be explained by the transformation of hydrogenation sites to desulfurization sites by the perpendicular adsorption of MPi.

Appendix A. Supplementary data

Supplementary data associated with this article can be found, in the online version, at doi:10.1016/j.jcat.2009.03.011.

References

[1] M. Houalla, N.K. Nag, A.V. Sapre, D.H. Broderick, B.C. Gates, AIChE J. 24 (1978) 1015.
[2] M.J. Girgis, B.C. Gates, Ind. Eng. Chem. Res. 30 (1991) 2021.
[3] H. Topsøe, B.S. Clausen, F.E. Massoth, Hydrotreating Catalysis, Science and Technology, Springer, Berlin, 1996.
[4] D.D. Whitehurst, T. Isoda, I. Mochida, Adv. Catal. 42 (1998) 345.
[5] T. Kabe, A. Ishihara, W. Qian, Hydrodesulfurization and Hydrodenitrogenation, Kodansha Ltd./Wiley-VCH, Tokyo/Weinheim, 1999.
[6] R. Prins, in: G. Ertl, H. Knözinger, F. Schüth, J. Weitkamp (Eds.), Handbook of Heterogeneous Catalysis, second ed., Wiley-VCH, Weinheim, 2008, p. 2695.
[7] A. Röthlisberger, R. Prins, J. Catal. 235 (2005) 229.
[8] T. Kabe, A. Ishihara, Q. Zhang, Appl. Catal. A 97 (1993) L1.
[9] F. Bataille, J.L. Lemberton, P. Michaud, G. Pérot, M.L. Vrinat, M. Lemaire, E. Schulz, M. Breysse, S. Kasztelan, J. Catal. 191 (2000) 409.
[10] M. Macaud, A. Milenkovic, E. Schulz, M. Lemaire, M. Vrinat, J. Catal. 193 (2000) 255.
[11] M. Egorova, R. Prins, J. Catal. 225 (2004) 417.
[12] B.C. Gates, H. Topsøe, Polyhedron 16 (1997) 3213.
[13] M. Houlla, D.H. Broderick, A.V. Sapre, N.K. Nag, V.H.J. de Beer, B.C. Gates, H. Kwart, J. Catal. 61 (1980) 523.
[14] T. Kabe, A. Ishihara, H. Tajima, Ind. Eng. Chem. Res. 31 (1992) 1577.
[15] V. Meille, E. Schulz, M. Lemaire, M. Vrinat, J. Catal. 170 (1997) 29.
[16] M. Daage, R.R. Chianelli, J. Catal. 149 (1994) 414.

[17] P. Kukula, V. Gramlich, R. Prins, Helv. Chim. Acta 89 (2006) 1623.
[18] X. Li, A. Wang, M. Egorova, R. Prins, J. Catal. 250 (2007) 283.
[19] H. Wang, R. Prins, J. Catal. 258 (2008) 153.
[20] Y. Sun, H. Wang, R. Prins, Tetrahedron Lett. 49 (2008) 2063.
[21] O. Levenspiel, Chemical Reaction Engineering, third ed., Wiley, 1998.
[22] J.C. DiCesare, L.B. Thompson, R.J. Andersen, J. Nail, Org. Prep. Proceed. Int. 32 (2000) 169.
[23] R.J.M. Voorhoeve, J.C.M. Stuiver, J. Catal. 23 (1971) 243.
[24] A. Wambeke, L. Jalowiecki, S. Kastelan, J. Grimblot, J.P. Bonnelle, J. Catal. 109 (1988) 320.
[25] M. Jian, R. Prins, Catal. Lett. 50 (1998) 9.
[26] P. Raybaud, J. Hafner, G. Kresse, S. Kasztelan, H. Toulhoat, J. Catal. 190 (2000) 128.
[27] H. Schweiger, P. Raybaud, H. Toulhoat, J. Catal. 212 (2002) 33.
[28] M. Sun, A.E. Nelson, J. Adjaye, J. Catal. 226 (2004) 32.
[29] E. Krebs, B. Silvi, P. Raybaud, Catal. Today 130 (2008) 160.
[30] M. Egorova, R. Prins, J. Catal. 221 (2004) 11.
[31] S. Kasztelan, D. Guillaume, Ind. Eng. Res. 33 (1994) 203;
S. Kasztelan, D. Guillaume, Ind. Eng. Res. 34 (1995) 1500.
[32] R.T. Hanlon, Energy Fuels 1 (1987) 424.
[33] J.V. Lauritsen, S. Helveg, E. Lægsgaard, I. Stensgaard, B.S. Clausen, H. Topsøe, F. Besenbacher, J. Catal. 197 (2001) 1.
[34] J.V. Lauritsen, M. Nyberg, J.K. Nørskov, B.S. Clausen, H. Topsøe, E. Lægsgaard, F. Besenbacher, J. Catal. 224 (2004) 94.
[35] P. Kukula, A. Dutly, H. Rüegger, R. Prins, Tetrahedron Lett. 48 (2007) 5657.
[36] M. Sun, A.E. Nelson, J. Adjaye, Catal. Today 105 (2005) 36.
[37] L. Qu, R. Prins, Appl. Catal. A 250 (2003) 105.
[38] X. Ma, K. Sakanishi, T. Isoda, I. Mochida, Energ. Fuel 9 (1995) 33.
[39] S.S. Katti, D.W.B. Westerman, B.C. Gates, T. Youngless, L. Petrakis, Ind. Eng. Chem. Process Des. Dev. 23 (1984) 773.
[40] M. Egorova, R. Prins, J. Catal. 241 (2006) 162.
[41] A. Logadottir, P.G. Moses, B. Hinnemann, N.-Y. Topsøe, K.G. Knudsen, H. Topsøe, J.K. Nørskov, Catal. Today 111 (2006) 44.
[42] M. Sun, A.E. Nelson, J. Adjaye, J. Catal. 231 (2005) 223.
[43] M. Egorova, R. Prins, Catal. Lett. 92 (2004) 87.
[44] Th. Weber, J.A.R. van Veen, Catal. Today 130 (2008) 170.
[45] X.Q. Yao, Y.W. Li, H. Jiao, J. Mol. Struct. THEOCHEM 726 (2005) 67.
[46] S. Cristol, J.F. Paul, E. Payen, D. Bougeard, J. Hafner, F. Hutschka, Stud. Surf. Sci. Catal. 127 (1999) 327.